

# ELECTRODICHROISM OF PURPLE MEMBRANE

## Ionic Strength Dependence

E. PAPP, G. FRICSOVSZKY, AND G. MESZÉNA

*Department of Atomic Physics, Eötvös University, 1088 Budapest, Puskin u. 5-7, Hungary*

**ABSTRACT** The dichroism of purple membrane suspension was measured in dc and ac electric fields. From these measurements three parameters can be obtained: the permanent dipole moment,  $\mu$ , the electrical polarizability,  $\alpha$ , and the retinal angle,  $\delta$ , (relative to the membrane normal). The functional dependence of the dichroism on the electric field is analyzed. There is a small decrease ( $\sim 2^\circ$ ) in retinal angle going from dark adapted to the light adapted form. No measurable difference in  $\mu$ ,  $\alpha$ , and  $\delta$  was found under the photocycle. The dichroism was measured in two different salt solutions (KCl and  $\text{CaCl}_2$ ) in the range 0–10 mM. The retinal angle increases from  $64^\circ$  to  $68^\circ$  with increasing ionic strength going through a minimum. This is attributed to the changing (decreasing) inner electric field in the membrane. The polarizability,  $\alpha$ , consists of two parts. One component is related to the polarization of the purple membrane and the second component to the ionic cloud. The second component decreases with ion concentration approximately as  $\kappa^{-3}$  ( $\kappa$  is the Debye parameter) in agreement with a model calculation for the polarization of the ionic cloud. The origin of the slightly ionic strength dependent permanent dipole moment is not well understood.

### INTRODUCTION

Electrooptical measurements on purple membrane (pm) suspensions were made by several authors (1–8). These measurements can be divided into two groups. In the first group (1, 4, 5) a strong but sufficiently short ( $\sim 10 \mu\text{s}$ ) electric impulse is applied. It is supposed that the duration of the impulse is so short, that it cannot cause substantial rotation of pm, and thus the observed electrooptical effect are assumed to reflect internal, conformational changes in the pm, caused by the electric field. In the second group (2, 3, 6–8) a moderate but longer ( $\sim 1 \text{ s}$ ) electric field was applied to pm suspension. In that case, time is long enough to allow a steady-state redistribution of pm, leading to an optically anisotropic medium.

In his experiment Keszthelyi (2) found that the pm has a permanent electric dipole moment ( $\mu$ ) pointing perpendicular to the membrane plane. Because of this dipole moment a low dc electric field ( $\sim 10 \text{ V/cm}$ ) can highly orient the pm in the suspension perpendicular to the field (dc orientation). This method of orientation was used to study the transient electric signal of proton movement during the photocycle (9).

Kimura et al. (3, 8) observed a change in alignment going from low to higher frequency of the applied field. Above  $\sim 100 \text{ Hz}$  the membranes will align with their plane parallel to the field (ac orientation). This observation has been attributed to the polarization of the membrane interface.

In this paper we report the results of dc and ac electrochromism measurements on pm mainly in steady-

state conditions. First the experimental setup is outlined. In Results the experimental data are compared with theory, and the effect of several factors on electrochromism (light-dark adaption, photocycle, ionic strength) is given. At the end we discuss our results and compare with other results.

### MATERIALS AND METHODS

Suspensions of purple membrane sheets prepared from *Halobacterium halobium* (Strain JW-3) were a gift from the Institute of Biophysics, Biological Research Center, Hungarian Academy of Science, Szeged. The original suspension, which contained  $\sim 100 \mu\text{mol/l}$  bacteriorhodopsin (BR), was stored at  $4^\circ\text{C}$  and was used within 3 mo. To make the effect of polydispersity less significant the suspensions were filtered under  $\text{N}_2$  atmosphere by nuclear filters (pore sizes 1.0 and  $1.27 \mu\text{m}$ ; JINR, Dubna, USSR) and diluted to the final concentration ( $\sim 5 \cdot 10^{-6} \text{ mol/l}$ ) with the appropriate salt solutions. After dilution the absorbances were  $0.5\text{--}0.8 \text{ cm}^{-1}$ .

The two main electrodes were platinized platinum sheets ( $15 \times 4 \text{ mm}$ ) cemented on glass. Two potential measuring electrodes were placed between the current-electrodes slightly above the measuring light path. They were made from platinum wires ( $0.1 \text{ mm}$  diam) in glass capillaries and they were platinized, too. The electrodes for the measurements in distilled water or in salt solutions of low concentration were freshly prepared or renewed by standard procedure. For light-adaptation and photocycle excitation of the BR a window was made on the bottom side of the cuvette, allowing illumination of the suspension perpendicular to the measuring light. The cuvette was thermostatted at  $25^\circ\text{C}$ .

The electric dichroism was generated either by a train of  $2 \text{ kHz}$  sinusoidal-waves or a pair of dc-impulses with opposite sign (duration of impulses  $1 \text{ s}$ ). Triggering signals from a Timer (Biol. Res. Center, Hung. Acad. of Sci., Szeged) allowed the simultaneous measurement of the transmitted light intensity and the electric potential between the electrodes from which the dichroism and the field strength were calculated. The time-dependence of the signals was measured — after compensating and amplifying — by a transient recorder (NEO-200, CRIP, Hungary).

## THEORY

The theory of electrooptical effects was given by Shah (10). We reproduce here the main results of this theory applied to the electrochromism of purple membrane.

Suppose that the pm fragments have an electric dipole moment,  $\mu$ , pointing to the direction of the membrane normal (Fig. 1) and electrical polarizability ( $\alpha_1$  along the normal,  $\alpha_2$  perpendicular to it and  $\alpha_2 > \alpha_1$ ). The angle between the retinal and the membrane normal is  $\delta$ . In a suspension the pm fragments will be thermally randomized and in spite of the retinal fixed orientation in the membrane, the absorption of polarized light is isotropic, independent of polarization. In an electric field the permanent and induced dipole moments interact with the field, leading to a partial alignment of membranes against thermal randomization. This results in an anisotropic absorption (electric dichroism). The relative absorption change ( $S_e$ ) can be given by

$$S_e = (A_e - A)/A = \frac{1}{2}(3 \cos^2 \delta - 1)(3 \cos^2 \sigma - 1)\phi, \quad (1)$$

where  $\sigma$  is the angle between the measurement polarized light electric vector and the external electric field,  $E$ . Here  $\phi$  is the orientation factor defined by

$$\phi = \frac{1}{2} \langle 3 \cos^2 \theta - 1 \rangle, \quad (2)$$

where  $\theta$  is the angle between the electric field and the membrane normal (Fig. 1).  $\langle \rangle$  means an average over the Boltzmann distribution function.  $\phi$  can be given by

$$\phi(\beta, \gamma) = \frac{3}{2} \frac{\int_{-1}^1 x^2 \exp(\beta x - \gamma x^2) dx}{\int_{-1}^1 \exp(\beta x - \gamma x^2) dx} - \frac{1}{2}, \quad (3)$$

where

$$\begin{aligned} \beta &= \mu E / (kT) = \beta_0 E \\ \gamma &= (\alpha_2 - \alpha_1) E^2 / (2kT) = \gamma_0 E^2 \\ x &= \cos \theta \end{aligned} \quad (4)$$

and  $k$  is the Boltzmann constant and  $T$  is the absolute temperature.

In the above considerations it is tentatively assumed that the external electric field does not cause any internal changes in the pm molecular structure, its effect is only a pure rotational redistribution of the pm fragments. In that case it follows from Eq. 1 for  $S_{\parallel}$  ( $\sigma = 0$ ) and  $S_{\perp}$  ( $\sigma = 90^\circ$ ):

$$S_{\parallel} + 2 S_{\perp} = 0. \quad (5)$$

## RESULTS

The previous theoretical results relate to steady state conditions. When the electric field is suddenly switched on

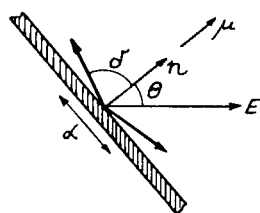


FIGURE 1 The direction of the retinal ( $\delta$ ), the electric dipole moment ( $\mu$ ) and the main polarizability ( $\alpha$ ) relative to the membrane normal ( $n$ ).  $E$  is the external electric field.

or off, before reaching the steady state there is a transient behavior of electrochromism. To describe the transient signal the rotational diffusion differential equation should be solved. There are two limiting cases for pm electrochromism. If  $\tau$  is the rotational diffusion time constant of a pm fragment (in our case  $\tau \sim 10$ – $100$  ms, see later), a frequency  $\nu_0$  can be defined:  $\nu_0 = 1/\tau$ . If  $\nu$  is the frequency of the electric field, the two limiting cases are: (a)  $\nu \ll \nu_0$ . The rotation of pm can follow the electric field. It is found experimentally that at low fields the polarizability is much smaller than the permanent dipole moment ( $\beta^2 \gg \gamma$ , see Eq. 4), the pm can be regarded as having only permanent dipole moment (with  $\gamma \approx 0$ ). This is called dc electrochromism. In our experiment it is realized with  $\nu \sim 1/2$  Hz. (b)  $\nu \gg \nu_0$ . In this case the pm cannot follow the rapid change of the electric field. The permanent dipole moment contribution (depending on  $E$ ) in Eq. 3 averages out to zero and only the polarization term remains. This is called ac electrochromism. In our experiment  $\nu = 2$  kHz was used. We found that in the range of  $\sim 0.5$  kHz  $< \nu < 100$  kHz, the ac electrochromism is practically independent of frequency. We used the effective value of  $E$  in Eq. 4, as the time average for the interaction energy.

The frequency dependence and transient behavior of electrochromism of pm was studied experimentally in detail by Kimura et al. (8). Thus, in the case of pure ac electrochromism it can be shown that the ratio of the areas above the rising curve and under the decaying curve of the dichroic signal should approach 1 as  $E$  goes to 0. This is supported by experiment (Fig. 2). In the case of dc electrochromism this ratio is 4 (data not shown).

## ac Electrochromism

First we would like to check to what extent are the previous relations fulfilled experimentally, namely the dependence on the polarization angle,  $\sigma$ , and on the electric field,  $E$ ,

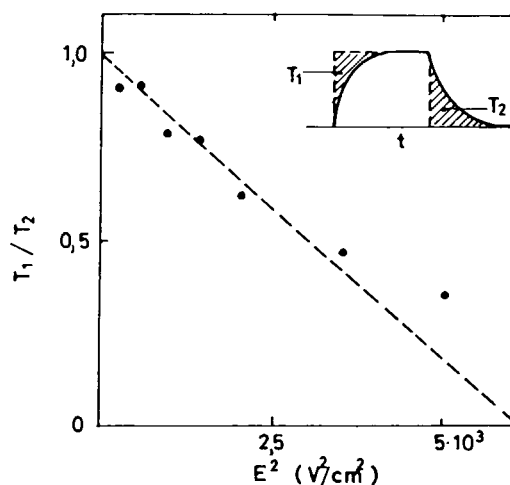


FIGURE 2 The ratio of the areas of ac dichroic signal as a function of the ac electric field squared. The insert shows the time dependence of the dichroic signal and the areas.

(Eqs. 1, 3, and 5). All measurements here were made on suspensions in distilled water and at  $\nu = 2$  kHz.

Fig. 3 shows the dependence of  $S_{\parallel}$  and  $S_{\perp}$  on the electric field. Evidently Eq. 5 is not fulfilled. This deviation may reflect an intrinsic change in the membrane caused by the electric field and/or an asymmetry around the field.

Light scattering can cause asymmetry and deviation from Eq. 5. Some details about light scattering are given in Appendix I.

In the derivation of Eqs. 1 and 5 it is assumed that the only effect of the electric field is a pure rotation of pm. If the electric field causes some change inside the membrane (which results e.g., in a change of absorption when the field is on), this effect has to be taken into account separately. A similar deviation was found by Tsuji et al. (5) who referred to this change as "chemical."

A sensitive way to present this deviation is the dependence of  $S_{\sigma}$  on the polarization angle,  $\sigma$ . According to Eq. 1 in the case of a pure rotation,  $S_{\sigma}$  depends on  $(3 \cos^2 \sigma - 1)$  linearly (at constant field, i.e., at constant  $\phi$ ) going through the origin. This plot is given in Fig. 4 for two different fields. As can be seen the dependence is almost linear, but the line does not go through the origin. There are two deviations: a parallel shift of the line and an increase at  $\sigma = 0^\circ$  and  $\sigma = 90^\circ$ . The first is an isotropic part (not dependent on  $\sigma$ ) and the second is an anisotropic part of the deviation. As can be seen from Fig. 4 a parallel shift of the measured  $S_{\sigma}$  to the origin restores the validity of Eq. 5 to a high degree. The origin of these isotropic and an anisotropic deviations is not well understood. Tentatively we attribute them to a "chemical" change and light scattering, respectively. To get the rotational part of  $S_{\sigma}$ , we will make a

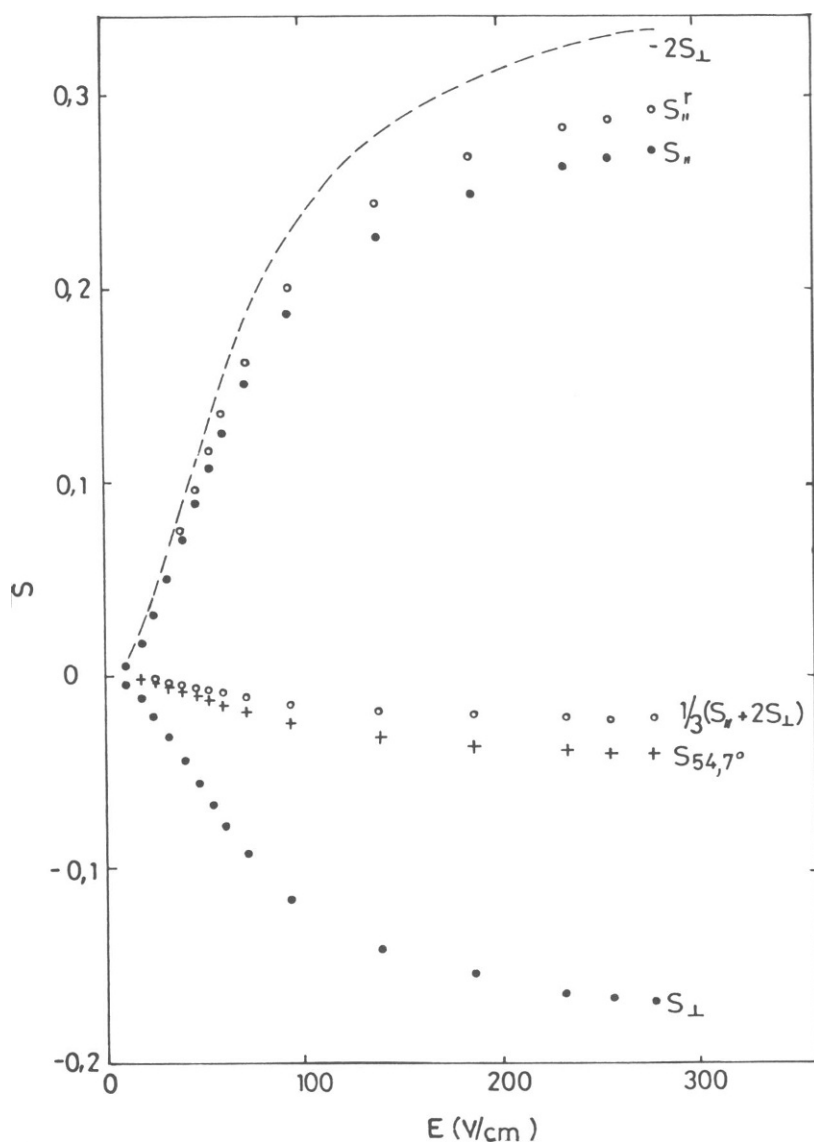


FIGURE 3 Electric field dependence of experimental dichroism at  $\sigma = 0$  ( $S_{\parallel}$ ),  $\sigma = 90^\circ$  ( $S_{\perp}$ ), and at  $\sigma = 54.7^\circ$  magic angle ( $S_{54.7}$ ). The  $-2S_{\perp}$  curve (dashed line) is higher than  $S_{\parallel}$ , showing a deviation from Eq. 5 (pm suspension in distilled water.)

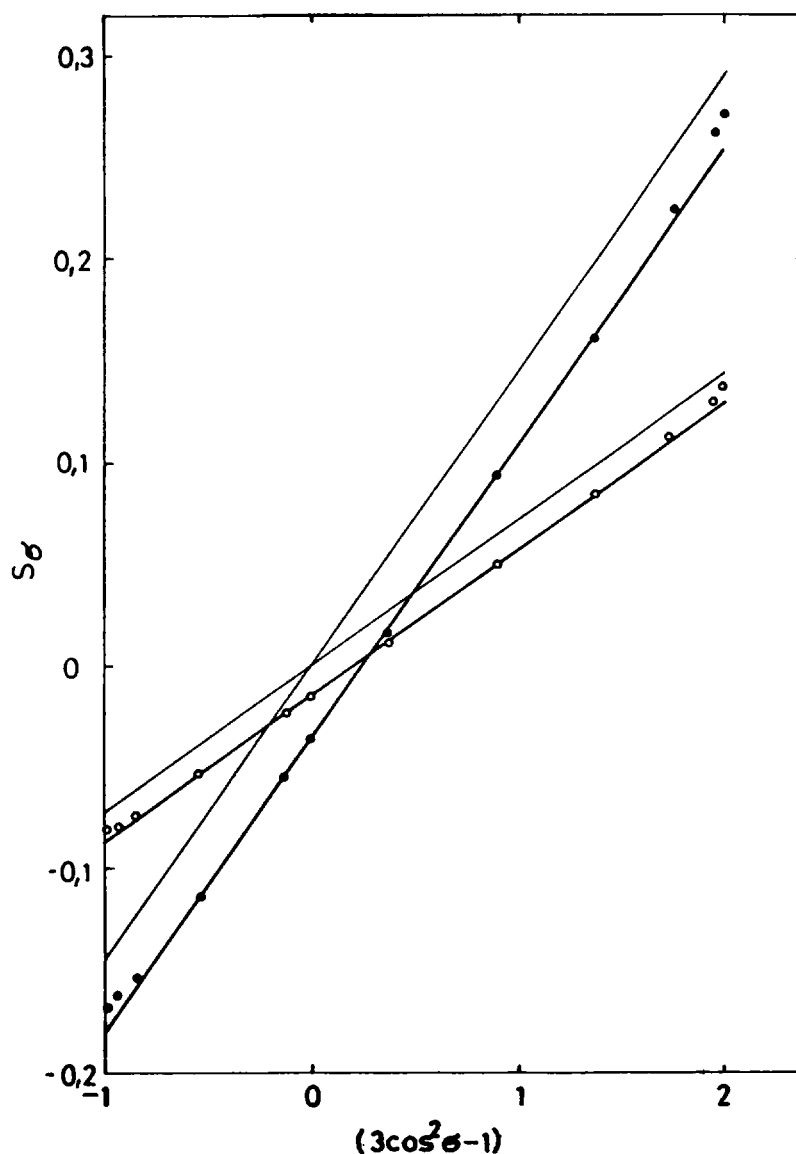


FIGURE 4 The dependence of electric dichroism on the polarization angle factor at two different electric fields ( $\circ E = 73$  V/cm  $\bullet E = 289$  V/cm). The light straight lines are a parallel shift to the origin of the heavy lines going through the experimental points (pm suspension in distilled water).

correction to the measured  $S_{\parallel}$  (see also reference 7)

$$S'_{\parallel} = S_{\parallel} - \frac{1}{3}(S_{\parallel} + 2S_{\perp}). \quad (6)$$

From the ac electrochromism measurements, two parameters, the retinal angle,  $\delta$ , and the polarizability,  $\gamma_0$ , can be obtained by fitting to Eq. 1. The corrected  $S'_{\parallel}$  values were used to the fit. If Eq. 1 holds with a constant retinal angle,  $\delta$ , then  $S'_{\parallel}$  should depend linearly on  $\phi$ . This is not the case as it is shown in Fig. 5. The fit was made to the lower electric field values of  $S'_{\parallel}$ . There is a systematic deviation from Eq. 1 as if the retinal angle,  $\delta$ , were increasing at higher orienting fields.

As the experimental  $S'_{\parallel}$  data cannot be fitted to  $\phi$  in the whole range, first we will fit at lower fields. It is shown in Appendix II that  $\phi$  (Eq. 3) can be series expanded in

powers of  $E^2$ . To get the two parameters  $\delta$  and  $\gamma_0$  it is necessary to go up to the  $E^4$  term in the series expansion. This means that  $S'_{\parallel}/E^2$  should be a straight line as a function of  $E^2$  at lower fields

$$S'_{\parallel}/E^2 = a_1 + a_2 E^2 \quad (7)$$

and using Eq. A2.4 with  $\beta = 0$  we get

$$\begin{aligned} \gamma_0 &= -21a_2/(2a_1) \\ g &= 3 \cos^2 \delta - 1 = 5a_1^2/(7a_2). \end{aligned} \quad (8)$$

The experimental  $S'_{\parallel}$  values show this behavior and the  $\delta$  and  $\gamma_0$  parameters derived by this way agree quite well with the presentation shown in Fig. 5 (lower curve). In the following the parameters derived by this way will be

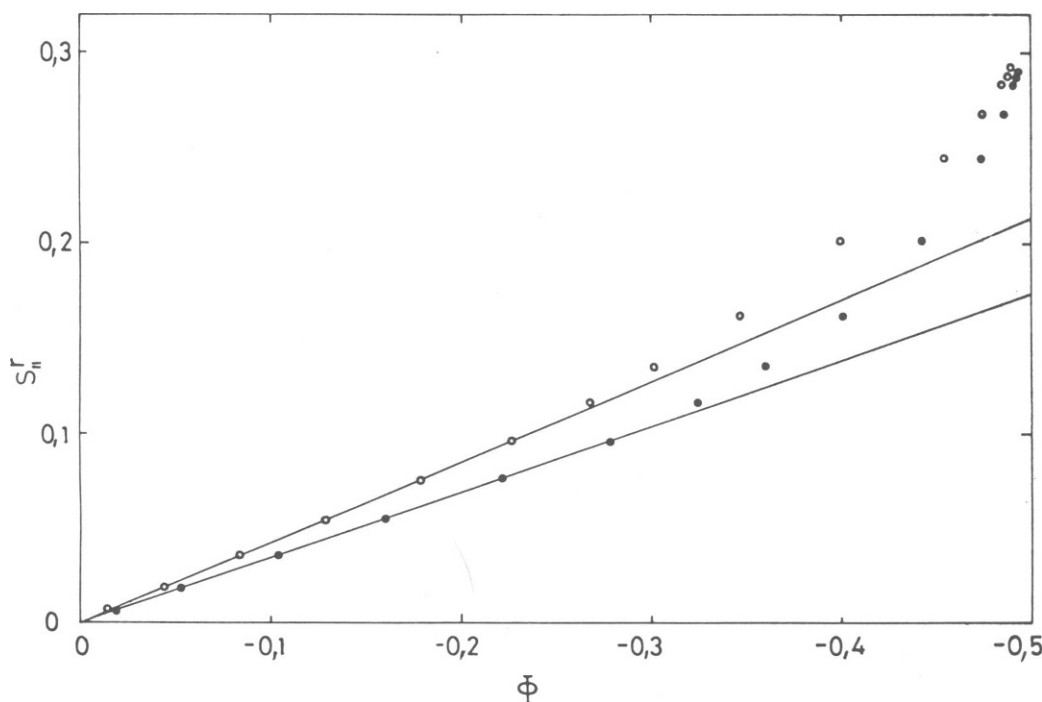


FIGURE 5 Lower curve (●):  $S_1''$  vs.  $\Phi$  representation with parameters  $\delta = 62.2^\circ$  and  $\gamma_0 = 15.1 \cdot 10^{-4} \text{ cm}^2/\text{V}^2$ . Upper curve (○): the effect of polydispersity (see the text). (pm suspension in distilled water).

denoted as experimental by  $g^e$  and  $\gamma_0^e$ . We emphasize that the correction made to  $S_1$  in Eq. 6 does not make much difference in the behavior of  $S_1$  as a function of  $E$ .

The polydispersity of the pm fragments can cause a deviation from Eq. 3. The point is that the smaller fragments have smaller  $\gamma_0$  and they will orient at higher fields. We will treat the polydispersity in the following way (see Appendix II also). Using Eqs. 7 and A2.7 we get

$$\begin{aligned}\gamma_0^e &= \overline{\gamma_0^2} / \overline{\gamma_0} \\ g^e &= g \cdot (\overline{\gamma_0^2} / \overline{\gamma_0}^2)\end{aligned}\quad (9)$$

(where the bar means average over the size distribution), or with the mean square deviation of  $\gamma_0$ :

$$g/g^e - 1 = (\overline{\gamma_0^2} - \overline{\gamma_0}^2) / \overline{\gamma_0}^2 > 0 \quad (10)$$

Eqs. 9 and 10 clearly show the effect of polydispersity on the experimental determination of the parameters  $\gamma_0^e$  and  $g^e$ . For a monodisperse sample  $\overline{\gamma_0^2} = \overline{\gamma_0}^2$  (and only for this case) and then  $\gamma_0^e = \gamma_0$  and  $g^e = g$ . But for polydisperse sample  $\gamma_0^e$  and  $g^e$  depend on the  $p(\gamma_0)$  distribution and in general  $\gamma_0^e > \gamma_0$  and  $g^e < g$ .

We checked the polydispersity of the purple membrane suspension by measuring the relaxation of the dichroic signal after switching off the orienting ac field. The relaxation can be fitted by two time constants (except at high electric fields and lower ionic strength, where at least three time constants appear). The amplitudes of these two components depend on the field, the faster component increasing with the field. We concluded from these mea-

surements that our sample consists mainly of two components with different membrane sizes. One component has a relaxation time  $\tau_1 \sim 100$  ms and the other  $\tau_2 \sim 15$  ms. From Perrin's formulae we get for the membrane diameters  $d_1 \sim 1.1 \mu\text{m}$  and  $d_2 \sim 0.6 \mu\text{m}$ . At higher fields (and higher ionic strength), where the orientation is almost complete, the relative amplitudes are  $p_1 \sim 0.6$  and  $p_2 \sim 0.4$ . The change of the relative amplitudes with the electric field can be accounted for by the polydispersity.

It was mentioned earlier that the pm suspension was fractionated by nuclear filters. Electronmicroscopy shows that pm fragments are not circular but elongated or irregular. Most of the population with larger size belongs to  $\sim 1\text{--}1.3 \mu\text{m}$  diam, corresponding to the used nuclear filters. The two time constants observed in relaxation may reflect partly the larger and smaller size of one pm fragment. We believe that the relaxation gives more reliable statistics for polydispersity than electron microscopy.

With the above values the effect of polydispersity on the measured  $\gamma_0^e$  and  $g^e$  can be taken into account. Assuming a  $\gamma_0 \sim d^2$  dependence and that  $g$  (retinal angle) does not depend on the membrane size,  $\gamma$  and  $g$  can be calculated using Eq. 9. The result is shown in Fig. 5 (upper curve).

The fit is better with polydispersity, but a deviation remains at higher fields. We attribute this deviation to an increase in the retinal angle with the orienting ac electric field. For the data shown in Fig. 5 we get for  $g^e = -0.348$  ( $\delta = 62.2^\circ$ ), after correction for polydispersity  $g = -0.431$  ( $\delta = 64.2^\circ$ ) and at high fields  $g' = -0.6$  ( $\delta = 68.6^\circ$ ). The electric field effect on the retinal angle is a  $4^\circ$  increase (the

retinal turns to the membrane plane) at an ac field of 280 V/cm. Later we show that this electric field effect on retinal angle disappears with increasing ionic strength.

A few further remarks: With the given polydispersity Eq. 10 cannot be fulfilled without assuming a retinal angle increase. The observed third time constant in the ms range may correspond to the retinal angle increase relaxation. In the following we give the polydispersity corrected values for  $g$ ,  $\gamma_0$ , and  $\beta_0$ , furthermore  $\gamma_0$  and  $\beta_0$  are calculated for the larger size and denoted by  $\gamma_{01}$  and  $\beta_{01}$ .

### Electrodichroism in dc Field

Measurement of electrodichroism in dc fields should yield parameters  $\beta_0$  and  $\delta$ . It can be shown that the contribution of polarizability ( $\gamma_0$ ) is negligible at low dc electric fields (in the range of a few V/cm). The data reduction can be done similarly as in ac measurements using Eq. A2.4 with  $\gamma_0 = 0$ . It turns out, that the retinal angle determined from dc measurements is much smaller than the value derived from the ac dichroism data. A similar problem was found by Kimura et al. (3) and Barabás et al. (7). Purple membrane fragments have net negative electric charge and in dc electric field this causes an electrophoretic movement of the membranes. The translational electrophoretic movement disturbs the free rotation of the pm and causes a distortion of the electric dichroism measurements. To avoid this problem we used the data in the lowest order in Eq. A2.4 (i.e., the linear part in  $E^2$  of the measured  $S_1$ ). This allowed the determination of only one parameter, namely  $\beta_0$ ; for  $\delta$  we used the value derived from the ac measurement. But there is no guarantee that this procedure eliminates the electrophoretic distortion.

The electrophoretic distortion is much less serious in ac electrochromic measurements. Probably at 2 kHz frequencies and above, the pm cannot move electrophoretically and the disturbing hydrodynamic forces are negligible. This is supported by the observation that the electrochromic signal is constant in the frequency range 2–20 kHz at constant amplitude of the ac electric field. If electrophoresis disturbed the signal, it should be frequency dependent in this range, too.

### Light and Dark Adaptation

Most of our measurements were made on light adapted (LA) pm but in a few cases we measured dark adapted (DA) pm with low measuring light intensity, to check whether the retinal angle,  $\delta$ , and perhaps  $\gamma_0$  and  $\beta_0$  change with light-dark adaptation. We found (see later, Fig. 7) that  $\delta$  increases by  $\sim 2^\circ$  in the dark adapted form at low ionic strength. This increase is  $< 1^\circ$  at higher ionic strength (1 mM KCl or  $\text{CaCl}_2$ ).

The observed changes of  $\gamma_0$  and  $\beta_0$  with light-dark adaptation are within experimental uncertainties (Figs. 6 and 9). We can state only that there can be a slight increase of  $\gamma_0$  in the dark adapted form.

### Effect of the Photocycle on $\delta$ , $\gamma_0$ , and $\beta_0$

In these measurements the actinic light exciting the photocycle was perpendicular to both the absorption measuring light and the orienting electric field. For a given orienting field we measured the absorption with the actinic light on (proton pump working) and without actinic light (no proton pump). The scattered light from the actinic light

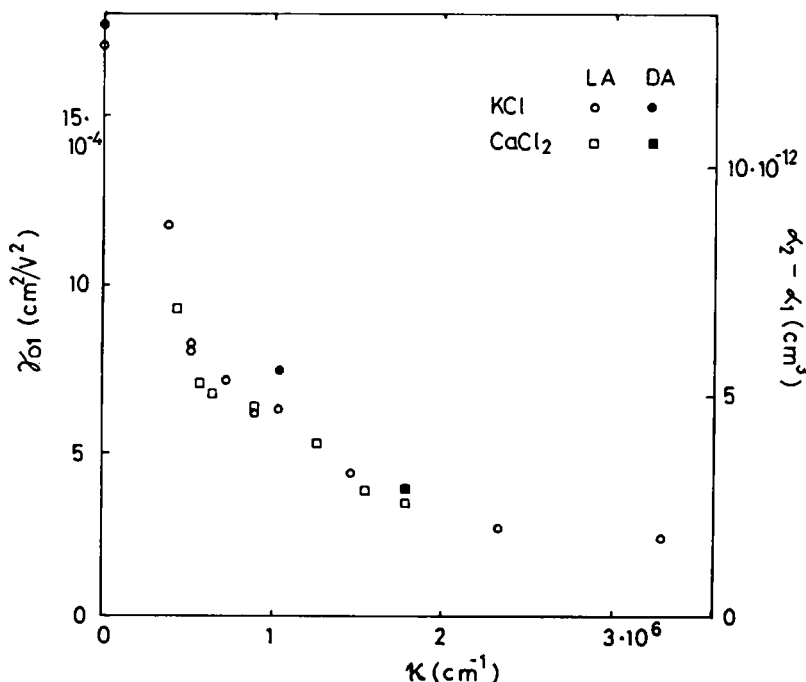


FIGURE 6 The dependence of the electrical polarizability of pm on the Debye-Hückel parameter,  $\kappa$ .

was measured separately and had to be taken into account. The absorption decreased from 0.34 to 0.307 under the actinic light for the parallel component ( $A_{\parallel}$ ) and to 0.316 for the perpendicular component ( $A_{\perp}$ ). This difference comes mainly from photoselection. From these data we estimated the photocycle working at a 30% power at the given actinic light intensity.

Within experimental uncertainties there was no detectable change in the electrochromism with and without the actinic light. We conclude that there is no essential change in  $\delta$ ,  $\gamma_0$ , and  $\beta_0$  if the proton pump is working.

#### Effect of Ionic Strength on $\delta$ , $\gamma_0$ , and $\beta_0$

Electrochromism was measured in KCl and CaCl<sub>2</sub> in the concentration range 0–10 mM and 0–2 mM. Above these concentrations detectable aggregation of pm occurred and the measurements were disregarded. In the highest salt concentration and at high ac orienting field 2–3°C temperature increase (measured with a Cu-constantan thermocouple) could be detected. This heating was not observable at lower fields and salt concentration. As  $\delta$ ,  $\gamma_0$ , and  $\beta_0$  are derived from the lower orienting field data, heating cannot effect these parameters.

The parameter,  $\gamma_0$ , and the polarizability ( $\alpha_2 - \alpha_1$ ) of the pm monotonically decrease with increasing ionic strength (Fig. 6). In this figure the data are given as a function of the Debye-Hückel constant,  $\kappa$ . As can be seen, the data are, within experimental uncertainties, on the same curve for both salts in this  $\kappa$ -representation. This supports the idea that the polarizability of pm originates in the electric polarization of the ionic cloud around pm. A similar behavior was found by Kimura et al. (3, 8).

We found a retinal angle dependence on salt concentra-

tion. With increasing  $\kappa$  the retinal angle first decreases and then increases to a higher value of  $\sim 68^\circ$  at our highest salt concentration. This is shown in Fig. 7. The minimum in  $\delta$  at low salt concentration seems to be shifted a little for CaCl<sub>2</sub>, but the behavior is similar. From electrochromic measurements Kimura et al. (3, 8) reported a value of  $\delta \sim 70^\circ$  and Barabás et al. (7)  $\delta \sim 68^\circ$ . These measurements were made at relatively high ionic strength and these agree with our data at high  $\kappa$ . We attribute the  $\delta$  dependence on salt concentration mainly to an inner electric field variation with salt concentration i.e., to a screening effect. This will be discussed later. It was mentioned earlier that at lower ionic strength we see an increase of  $\delta$  at high orienting fields (Fig. 5). This effect disappears at high salt concentration and the data can be represented by a constant retinal angle after correction for polydispersity (Fig. 8).

Though the determination of the permanent dipole moment of pm is less certain because of disturbing electrophoresis, we found a weak ionic strength dependence of  $\beta_0$  and  $\mu$ . Fig. 9 shows this dependence of  $\beta_0$  after correction for polydispersity and for the larger pm fragments (diameter  $\sim 1.1 \mu\text{m}$ ) and the calculated permanent dipole moment per bacteriorhodopsin, assuming  $1.1 \mu\text{m}$  diam. We get higher values for KCl than for CaCl<sub>2</sub>.

#### DISCUSSION

In this section we would like to discuss mainly the following observed effects: the rather strong ionic strength dependence of the polarizability (Fig. 6); the behavior of the retinal angle with ionic strength and in higher orienting ac electric field (Figs. 7 and 5); the magnitude and origin of the permanent dipole moment of pm.

The comparison of our data on  $\alpha$  with other measure-

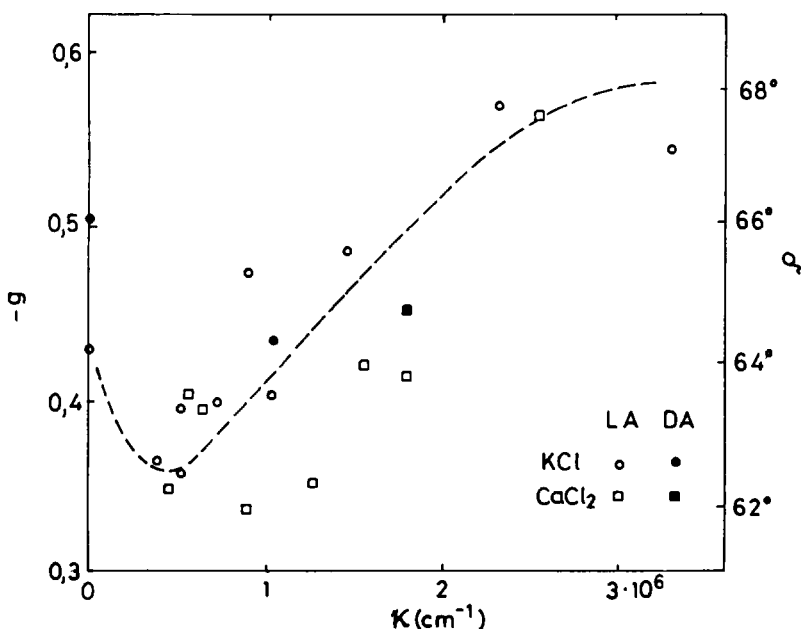


FIGURE 7 The dependence of the retinal angle,  $\delta$ , on the parameter  $\kappa$ .

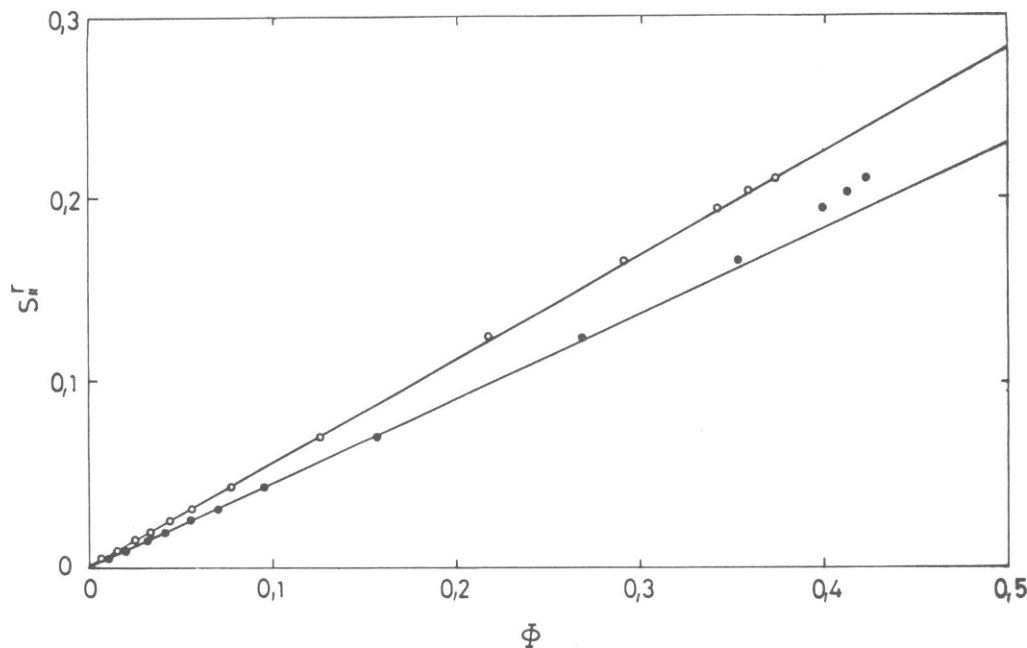


FIGURE 8 The same as Fig. 5 but for pm suspension in 5 mM KCl.

ments (3, 6–8) is difficult as these experiments were made with different membrane sizes and ionic strength. The polarizability depends on both of these parameters. Kimura et al. (3, 8) found a quite similar ionic strength dependence as our measurements give (Fig. 6). On this basis one can think that the polarizability of pm comes mainly from the electric polarization of the ionic cloud around the pm. A theoretical treatment of the polarization of ionic atmosphere around a long, infinitely thin, charged strip (membrane) of  $d$  width was given in (11). The result for the polarizability  $\alpha$ , parallel to the surface and along the width and for the unit length of the strip is

$$\alpha = \frac{2}{\epsilon} \left( \frac{\pi e Q}{kT} \right)^2 \frac{d^2}{\kappa^3} F(d\kappa), \quad (11)$$

where  $e$  is the elementary charge,  $Q$  is the charge of the strip per unit surface,  $\epsilon$  is the dielectric constant of the solution and  $F(d\kappa)$  is a slowly varying function approximating 1 if  $d \gg 1/\kappa$  (11). This result can be applied for a circular disk (e.g., for the pm) if the diameter  $d \gg 1/\kappa$ . In that case Eq. 11 gives for the polarizability of the disk

$$\alpha = \frac{1}{8\epsilon} \left( \frac{\pi e Q}{kT} \right)^2 \frac{d^2}{\kappa^3} F(d\kappa). \quad (11a)$$

(For comparison: the Debye length  $1/\kappa \approx 10$  nm for 1 mM KCl and  $d \sim 1,100$  nm for our pm). Eq. 11a gives a  $d^2$  and a  $\kappa^{-3}$  dependence for the polarizability at higher salt concentration. Fig. 10 shows the comparison of the measured  $\alpha$  (Fig. 6) and Eq. 11a at higher salt concentration. A  $\kappa^{-3}$  dependence is indeed observed. In Eq. 11a the only fitting parameter is  $Q$  if we take the pm size known. Assuming a disk of  $1.1 \mu\text{m}$  diam this gives for the net charge of pm  $\approx$

$2e/\text{BR}$ . The model of Engelman et al. (12) for the bacteriorhodopsin in purple membrane gives 14 positive and 19 negative charge for one BR at neutral pH distributed mainly near the surface of pm and partly inside the membrane. This gives five net negative charges/BR compared with our finding of two charges/BR. The difference can come partly from the charged lipid head groups.

The polarizability of the ionic cloud goes to zero as  $\kappa$  becomes large. But according to Fig. 10 we get a nonzero polarizability,  $\alpha_0 \sim 1.6 \cdot 10^{-12} \text{ cm}^3$ , at high  $\kappa$  value, too. This has to be attributed to an intrinsic polarizability of the purple membrane. It is not known what molecular groups in pm provide this intrinsic polarizability, but the changing retinal angle and permanent dipole moment (Figs. 7 and 9) suggest that the neighborhood of the retinal takes part in it. The small increase in polarizability on dark adaptation (Fig. 6) is probably due to a change in  $\alpha_0$  caused by the retinal conformational change.

Another point of Fig. 10 is the deviation of experimental polarizability from the expected theoretical value of Eq. 11a at higher  $F/\kappa^3$  (i.e., at lower ion concentration,  $<1$  mM for KCl). Numerical calculation (11) shows a rapid decrease of the function  $F(d\kappa)$ , but it occurs at a lower ionic strength than the above deviation. This deviation may reflect an intrinsic change in pm (e.g., internal electric field effect, see later) or some other ionic mechanism, different from the ionic cloud polarization.

To account for the observed change in retinal angle with ionic strength and ac field we take into account the effect of an internal electric field in pm. As the membrane is charged, with net negative charges located at the surface of the inside part of pm (12), at low ionic strength there will be a high electric field in the membrane, directed from



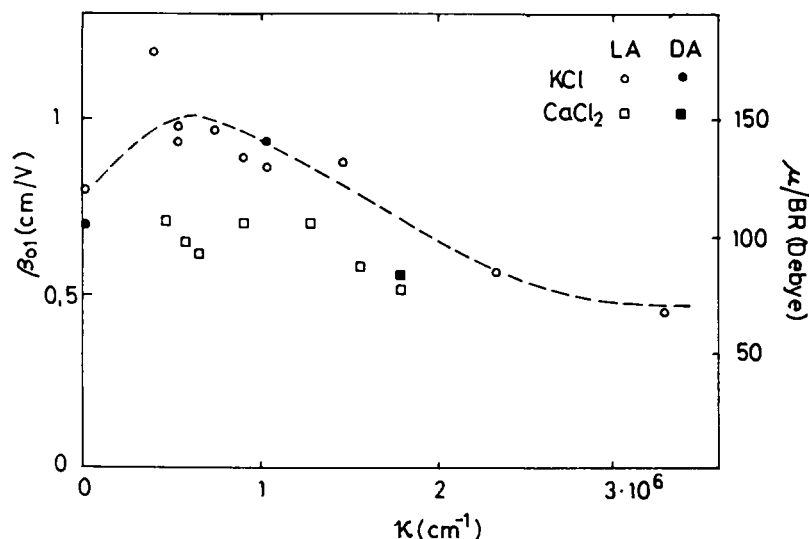


FIGURE 9 The dependence of the permanent electric dipole moment on the parameter  $\kappa$ .

outside to inside of pm. With increasing ionic strength the surface charges will be screened by the ionic cloud leading to the decrease of the internal field. This internal field can polarize the interior of pm, resulting in a change (decrease) of the retinal angle. The behavior of  $\delta$ ,  $\alpha_2 - \alpha_1$ , and  $\mu$  at  $\kappa < 10^6 \text{ cm}^{-1}$  (Figs. 6, 7, and 9) may reflect the same origin, namely the effect of the internal field.

In high orienting ac electric field the pm is parallel to the field. The ac field can interact with the retinal by

polarizing the environment of the retinal, leading to an increase of the retinal angle (Fig. 5). The effect of the orienting ac field on the retinal angle is opposite to the effect of the internal electric field due to membrane charges. At high ionic strength the internal field is low and the orienting ac field effect on the retinal disappears (Fig. 8). In this picture it is assumed that the retinal can turn more easily to the normal of the membrane than into the opposite direction (see also reference 5).

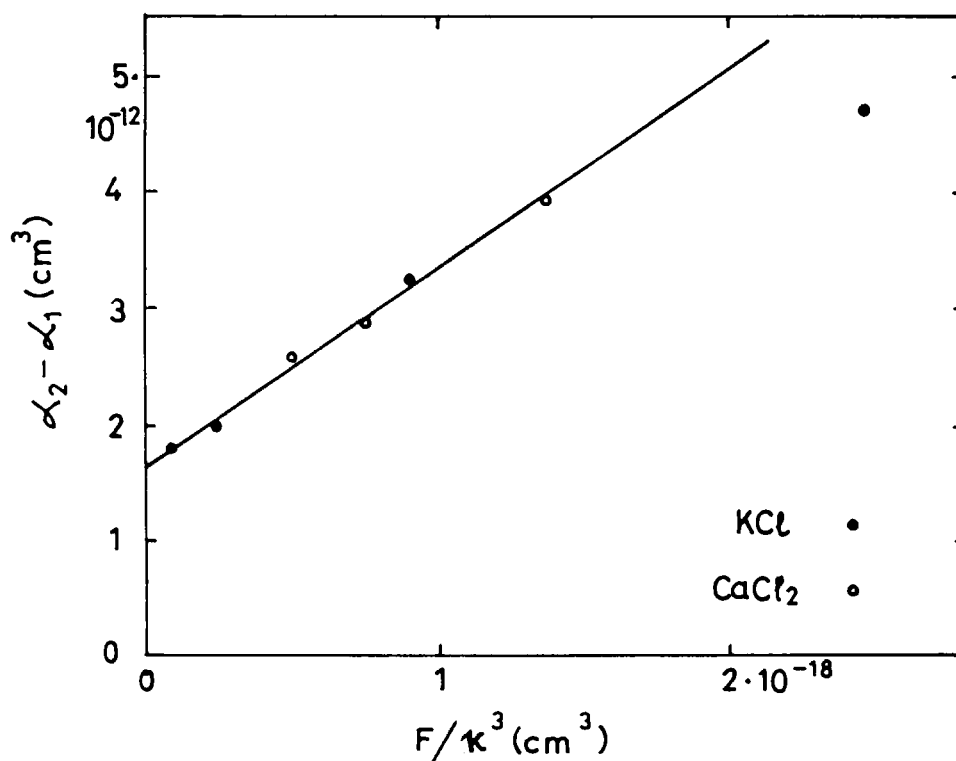


FIGURE 10 The polarizability as a function of  $F/\kappa^3$  (a fit to Eq. 11a).

There can be several contributions to the dipole moment of pm. The  $\alpha$ -helix of a protein has 3.4 D/residue (13). As BR in pm has an odd number of  $\alpha$ -helices (seven or five, see references 12 and 14), only one helix gives a contribution. Taking 20–25 residues in a helix we get 70–85 D dipole moment for one BR. Another contribution can come from the membrane charges, but to estimate this a detailed knowledge of the charge distribution would be needed. The internal electric field due to membrane charges can polarize the interior of the membrane giving the third part of the dipole moment. The ionic cloud and hydrodynamic effects can contribute to the dipole moment. To estimate the resulting dipole moment is a complicated problem. The observed dipole moment at high ionic strength is  $\sim 70$  D (Fig. 9) and this can be accounted for by the  $\alpha$ -helix contribution. The changes in the dipole moment at lower ionic strength can originate in the membrane charges and internal electric field effect. It is known (7) that at lower pH the dipole moment decreases and even changes sign. This is probably caused by the change of the membrane charges with pH.

No essential change in permanent dipole moment was found in this work under photocycle (see Results). A rather large decrease (35%) in dipole moment under photocycle was reported by Kimura et al. (8). The origin of contradiction in these two experimental observations is not known for us. We believe that we took properly into account the disturbing actinic light scattering to get reliable data for the dipole moment. Furthermore, it would be very difficult to understand such a big effect of photocycle on the permanent dipole moment.

Within experimental uncertainties ( $\sim 1^\circ$ ) we could not detect a change in retinal angle under photocycle. Two points have to be emphasized here. Electrochromism at 575 nm measures mainly the noncycling retinals and it gives the angle between the retinal's transition moment and the membrane normal. Consequently a possible rotation of the retinal (or bacteriorhodopsin) around the membrane normal under photocycle cannot be detected by this method. Light-activated rotation of bacteriorhodopsin was reported by Ahl and Cone (15).

## APPENDIX I

### Effect of Light Scattering on Electrochromism

The effect of light scattering on electrochromism measurements is briefly analyzed. If light scattering is present (as it always is), its effect is to increase the measured absorption of the sample. If  $A$  is the real absorption of the unoriented suspension and  $a$  is the apparent absorption caused by light scattering and  $A_\parallel$ ,  $a_\parallel$  are the same for oriented pm in electric field then the measured light intensities are

$$\begin{aligned} I &= I_0 \exp(-A - a) \\ I_\parallel &= I_0 \exp(-A_\parallel - a_\parallel). \end{aligned} \quad (\text{A1.1})$$

The measured value of  $S_\parallel$  is given by

$$S_\parallel = \frac{A_\parallel + a_\parallel - (A + a)}{A + a} = \frac{A_\parallel - A}{A} \cdot \frac{1 + (a_\parallel - a)/(A_\parallel - A)}{1 + a/A} \quad (\text{A1.2})$$

and the quotient  $S_\parallel/S_\perp$

$$S_\parallel/S_\perp = \frac{A_\parallel - A}{A_\perp - A} \cdot \frac{1 + (a_\parallel - a)/[\ln(I/I_\parallel) - (a_\parallel - a)]}{1 + (a_\perp - a)/[\ln(I/I_\perp) - (a_\perp - a)]}. \quad (\text{A1.3})$$

In Eq. A1.3 the first factor equals  $-2$  in the case of a pure rotation and the second factor gives the correction due to light scattering. Light scattering affects the quotient  $S_\parallel/S_\perp$  only if it is polarization angle dependent i.e., if  $a_\parallel$ ,  $a_\perp \neq a$ .

Measurements were made at  $\lambda = 725$  nm with the same electrochromism experimental set up. The result (Fig. 11) is similar to the electrochromism at  $\lambda = 575$  nm (see Fig. 3) but the parallel component decreased and the perpendicular component increased. If we assume that at  $\lambda = 725$  nm we have only light scattering i.e., there is no absorption by the pm at this wavelength, then Fig. 11 gives  $a_\parallel = a$  and  $a_\perp = a$  (see Eq. A1.2). In that case this result can be used to check Eq. A1.3, but the light scattering components  $a$  and  $a_\parallel$  have to be extrapolated to  $\lambda = 575$  nm. The light scattering is strongly particle size ( $d$ ) dependent. For small particle ( $d \ll \lambda$ ) we expect a Rayleigh  $\lambda^{-4}$  dependence, but for particle  $d \sim \lambda$ , as in the case of pm, a weaker dependence  $\lambda^{-2}$  would be appropriate. For both  $\lambda$ -dependence the calculated quotient according to Eq. A1.3 is shown in Fig. 12 with the observed  $S_\parallel/S_\perp$  values at  $\lambda = 575$  nm. As it is seen the  $\lambda^{-4}$  dependence would account for the observed deviation of  $S_\parallel/S_\perp$  from the ideal  $-2$  value but the  $\lambda^{-2}$  dependence is too weak and its effect is negligible.

We would like to make two further remarks. In the above consideration, it was assumed that the pm absorbs no light at  $\lambda = 725$  nm. A very small absorption (of the order of 1% or less of its maximum absorption at  $\lambda = 570$  nm) through electrochromism could account at least partly for the observed anisotropy at  $\lambda = 725$  nm (Fig. 11).

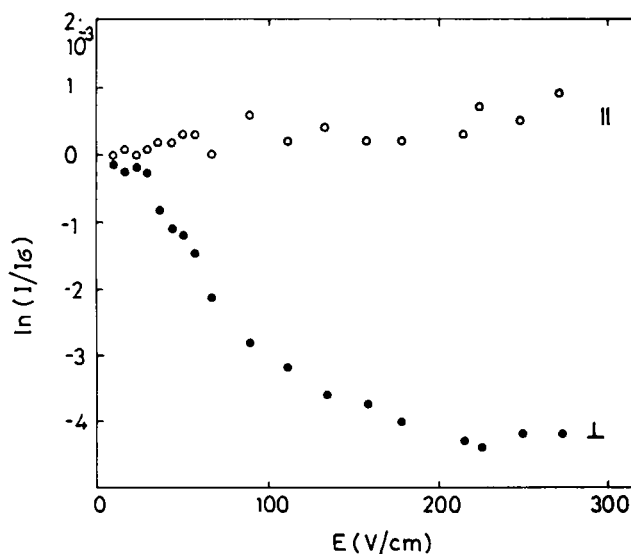


FIGURE 11 Electrochromism at  $\lambda = 725$  nm.

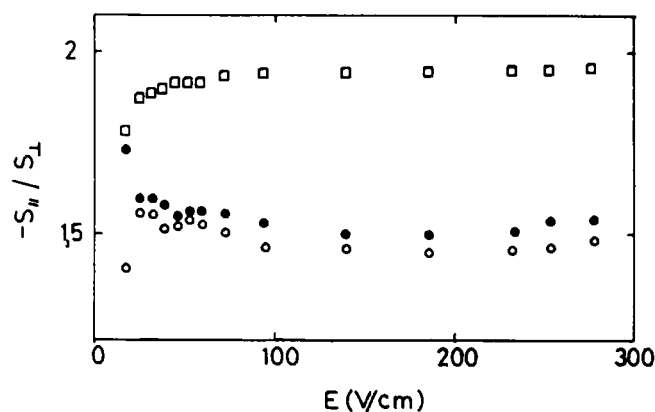


FIGURE 12 Deviation of  $-S_{||}/S_{\perp}$  from the expected ideal 2 value: ● experimental points measured at  $\lambda = 575$  nm, ○, □ corrected values for light scattering assuming a  $\lambda^{-4}$  and  $\lambda^{-2}$  dependence, respectively.

According to Eq. A1.2  $S_e$  can be split into two terms

$$S_e = \frac{\Delta A_e}{A + a} + \frac{\Delta a_e}{A + a}. \quad (\text{A1.4})$$

It seems to us that light scattering, the second term in Eq. A1.4, cannot cause an isotropic shift in  $S_e$  as is observed (see Fig. 4).

There is some uncertainty in these considerations: the role of light scattering, polarization angle dependence, isotropy (chemical) shift. We need more information about polarized light scattering on pm but our present experimental set up is not very suitable for sensitive light scattering measurements. The question clearly needs further investigation.

## APPENDIX II

### Series Expansion of $\phi$ and Polydispersity

In many cases it is not possible to get experimental data in the whole range of  $E$  to compare with the function  $\phi$ . Instead this comparison has to be made at lower fields with a series expansion of  $\phi$ . An expansion of  $\phi$  was given by Shah (10) but in his expansion some terms are missing. As in the literature this expansion is frequently used, we give here a short derivation.

To get an expansion of  $\phi$  in powers of  $E^2$  we expand in Eq. 3 only  $\exp(-\gamma x^2)$

$$e^{\beta x - \gamma x^2} = e^{\beta x} (1 - \gamma x^2 + \frac{1}{2} \gamma^2 x^4 \dots)$$

and introducing

$$f_n(\beta) = \int_{-1}^1 x^n e^{\beta x} dx \quad (\text{A2.1})$$

we get

$$\phi = \frac{3 f_2}{2 f_0} \left[ \frac{1 - (f_4/f_2)\gamma + (f_6/f_2)\gamma^2/2 \dots}{1 - (f_2/f_0)\gamma + (f_4/f_0)\gamma^2/2 \dots} \right]. \quad (\text{A2.2})$$

A recursion formula can be given for the functions,  $f_n$

$$\begin{aligned} f_0 &= 2 \sinh \beta / \beta \\ f_2/f_0 &= 1 + 2/\beta^2 - 2 \coth \beta / \beta \\ f_4/f_0 &= 1 + (3 \cdot 4/\beta^2) f_2/f_0 - 4 \coth \beta / \beta \end{aligned} \quad (\text{A2.3})$$

Taking expansion of  $f_n/f_0$  we get with Eq. A2.2 for  $\phi$

$$\phi = \frac{1}{15} \beta^2 - \frac{2}{15} \gamma - \frac{2}{315} \beta^4 - \frac{4}{315} \beta^2 \gamma + \frac{4}{315} \gamma^2 \dots \quad (\text{A2.4})$$

The effect of polydispersity for ac electric dichroism (i.e.,  $\beta_0 = 0$ ) can be taken into account with a distribution function  $p(\gamma_0)$ . If  $p(\gamma_0)d\gamma_0$  gives the fraction of the sample with parameter  $\gamma_0$  in the range  $(\gamma_0, \gamma_0 + d\gamma_0)$ , then the mean values are

$$\begin{aligned} \int_0^\infty p(\gamma_0) d\gamma_0 &= 1 \\ \overline{\gamma_0} &= \int_0^\infty \gamma_0 \cdot p(\gamma_0) d\gamma_0 \\ \overline{\gamma_0^2} &= \int_0^\infty \gamma_0^2 \cdot p(\gamma_0) d\gamma_0. \end{aligned} \quad (\text{A2.5})$$

For  $\phi$  we get

$$\overline{\phi(E)} = \int_0^\infty p(\gamma_0) \cdot \phi(\gamma_0, E) d\gamma_0 \quad (\text{A2.6})$$

Using Eq. A2.4,  $\overline{\phi}$  can be expanded in power of  $E^2$ .

$$\overline{\phi} = -\frac{2}{15} \overline{\gamma_0} \cdot E^2 + \frac{4}{315} \overline{\gamma_0^2} \cdot E^4 \dots \quad (\text{A2.7})$$

The authors are very much indebted to Dr. Zs. Dancsházy for providing pm samples, to Prof. L. Keszthelyi and Dr. K. Barabás for interesting discussions and to Mrs. Papp and Mr. S. Hopp for technical assistance.

This work was supported in part by the Ministry of Education, Hungary under grant 24.3.151.

Received for publication 9 April 1984 and in final form 27 November 1985.

## REFERENCES

- Shinar, R., S. Druckman, M. Ottolenghi, and R. Korenstein. 1977. Electric field effects in bacteriorhodopsin. *Biophys. J.* 19:1-5.
- Keszthelyi, L. 1980. Orientation of membrane fragments by electric field. *Biochem. Biophys. Acta.* 598:429-436.
- Kimura, Y., A. Ikegami, K. Ohno, S. Saigo, and Y. Takeuchi. 1981. Electric dichroism of purple membrane suspension. *Photochem. Photobiol.* 33:435-439.
- Druckman, S., and M. Ottolenghi. 1981. Electric dichroism in the purple membrane of *Halobacterium halobium*. *Biophys. J.* 33:263-268.
- Tsuji, K., and E. Neumann. 1981. Structural changes in bacteriorhodopsin induced by electric impulses. *Int. J. Biol. Macromol.* 3:231-242.
- Todorov, G., S. Sokerov, and S. P. S. Stoylov. 1982. Interfacial electric polarizability of purple membranes in solutions. *Biophys. J.* 40:1-5.
- Barabás, K., A. Dér, Zs. Dancsházy, P. Ormos, L. Keszthelyi, and M. Marden. 1983. Electro-optical measurements on aqueous suspension of purple membrane from *Halobacterium halobium*. *Biophys. J.* 43:5-11.
- Kimura, Y., M. Fujiwara, and A. Ikegami. 1984. Anisotropic electric properties of purple membrane and their change during the photoreaction cycle. *Biophys. J.* 45:615-625.
- Keszthelyi, L., and P. Ormos. 1980. Electric signals associated with the photocycle of bacteriorhodopsin. *FEBS (Fed. Eur. Biochem. Soc.) Lett.* 109:189-193.

10. Shah, M. I. 1963. Electric birefringence of bentonite II. An extension of saturation birefringence theory. *J. Phys. Chem.* 67:2215–2219.
11. Papp, E. 1985. Polarizability of the ionic cloud around a charged membrane sheet. *Biophys. Chem.* 21:243–248.
12. Engelman, D. M., and G. Zaccai. 1980. Bacteriorhodopsin is an inside out protein. *Proc. Natl. Acad. Sci. USA.* 77:5894–5898.
13. Hol, W. G. J., L. M. Halie, and C. Sander. 1981. Dipoles of the  $\alpha$ -helix and  $\beta$ -sheet: their role in protein folding. *Nature (Lond.)*. 294:532–536.
14. Jap, B. K., M. F. Maestre, S. B. Hayward, and R. M. Glaeser. 1983. Peptide-chain secondary structure of bacteriorhodopsin. *Biophys. J.* 43:81–89.
15. Ahl, P. L., and R. A. Cone. 1984. Light activates rotations of bacteriorhodopsin in the purple membrane. *Biophys. J.* 45:1039–1049.